

# PV Module Optimum Operation Modeling

Adel El Shahat

*Engineering Science Department, Faculty of Petroleum & Mining Engineering  
Suez University, Egypt*

## Abstract

This paper proposes first photovoltaic (PV) module theoretical modeling based on the Schott ASE-300-DGF PV panel as a practical basis for checking and verifying the modeling process. This is done with the aid of an equivalent electric circuit with a diode and an electric model with moderate complexity. It is modeled at nominal conditions at 25°C, and 1 kW/m<sup>2</sup> with I-V curves at (0°C, 25°C, 50°C, 75°C), also power and irradiance. General modeling in more probable situations for variable values of temperature and irradiance is proposed using Artificial Neural Networks (ANN). The inputs of this model are Irradiance and Temperature; the outputs are: Module Voltage, Current, and Power. All characteristics are well depicted in 3-D figures. Then, it proposes the identification of the maximum power point (MPP) function for the (PV) module using a genetic algorithm (GA). This function efficiently picks the peaks of PV power curves as the objective function and two variables as arguments ( $V_{mp}$  and  $I_{mp}$ ) with nonlinear constraints and variables boundaries. This function generates reference values to drive the tracking system in the PV system at optimum operation and is deduced with the aid of ANN too. This is done with probable situations for various values of temperature and irradiance to obtain corresponding voltage and current at maximum power. The simulation results at MPP are well depicted in 3-D figures to be used as training or learning data for the ANN model. The results obtained are sufficiently accurate to apply the models to control the PV systems for tracking the optimal power points.

**Keywords:** Photovoltaic, Neural Network, maximum power, Genetic Algorithm, MATLAB

## 1. Introduction

Photovoltaic modules are becoming increasingly popular and are ideally suited for distributed systems. Recent studies show an exponential increase in the worldwide installed photovoltaic power capacity. There is ongoing research aimed at reducing costs and achieving higher efficiency. Photovoltaic panels do not have any moving parts, operate silently and generate no emissions. Another advantage is that

solar technology is highly modular and can be easily scaled to provide the required power for different loads [1, 2]. A significant amount of PV research focused on fundamental issues of performance and modeling is presented [3–6]. Since the power harvested from the photovoltaic module differs at various operating points, it is important that maximum power is obtained from the photovoltaic module [7–9]. A PV array is usually oversized to compensate for a low power yield during winter months. This mismatch between the PV module and load requires further oversizing of the PV array and thus increases overall system cost. To mitigate this prob-

\*Corresponding author

Email address: adel.elshahat@ieee.org,  
adel12029@yahoo.com (Adel El Shahat)

lem, a maximum power point tracker (MPPT) can be used to maintain the PV module's operating point at the MPP. MPPTs can extract more than 97% of the PV power when properly optimized [7], [10]. Solar-array modeling and maximum power point tracking are studied by comparing two neural networks (back-propagation; radial basis) and are evaluated by comparison with a conventional model [11]. Neural networks can be applied to model the I-V characteristics and maximum power points (MPPs) of photovoltaic (PV) panels. A genetic algorithms-based training scheme to search for the optimal number of radial basis functions using only the input samples of a PV panel is proposed [12]. Modeling and simulation of a photovoltaic panel based on a neural network and VHDL language is introduced. This is done with an experimental database of meteorological data (irradiation, temperature) and output electrical generation signals of the PV-panel (current and voltage) [13]. Comprehensive efforts aimed at photovoltaic arrays modelling, optimization and simulations for grid-connected system are investigated [14], [15]. The equation of the external voltage-current characteristic  $I(V)$  of a solar cell is determined using genetic algorithms based on isolated points of the characteristic with very good convergence [16]. A traditional modeling approach using the Sandia Photovoltaic Array Performance Model is compared with a new method of characterization using a recurrent neural network (RNN). This comparison serves to validate the accuracy of the new method in comparison to a widely accepted modeling technique. Modeling using an RNN may be advantageous when component models are not available [17]. A novel genetic algorithm for maximum power point tracking based on the photovoltaic cell model is carried out. This proposed technique permits verification of the linearity between voltage and optimal current [18]. A method which combines an artificial neural network and a genetic algorithm in determining the tilt angle for photovoltaic (PV) modules is presented. This is done with the Taguchi experiment as the learning data for an artificial neural network (ANN) model. The objective is to maximize the electrical energy of modules in Taiwan [19]. Modeling of the electrical current-voltage and power-voltage of the photovoltaic (PV) panel BP 3160W, using a new ap-

proach based on artificial intelligence, is presented. The electrical parameters of solar cells of the optimal PV panel are analyzed by the simulation programs carried out in MATLAB [20]. A new kind of BP neural network modeling method based on MEA, and used for photovoltaic battery modeling is introduced. In this model, MEA is used for neural network parameter optimization to overcome defects of the traditional BP neural network and to improve modeling accuracy and reliability [21]. The application of an advanced neural network based model of a module to improve the accuracy of the predicted output I-V and P-V curves and to keep account of the changes in all parameters at different operating conditions is investigated [22]. A new application of the ANN for modeling a Photovoltaic Thermal collector (PV/T) is presented, together with thermal and electrical modelling. Networks with different hidden layers are used for modeling and the performances evaluated using maximum correlation coefficient, minimum root mean square error and low coefficient of variance [23]. An efficient and accurate approach for the estimation of solar cell parameters using a hybrid genetic algorithm from the given voltage-current data is proposed. The hybrid genetic algorithm, which is based on the Genetic Algorithm (GA) and Nelder-Mead (NM) simplex search method, is proposed. MATLAB OPTIMTOOL is used to implement the proposed approach [24]. The influence of light intensity, day type, temperature, and season on photovoltaic power is analyzed. By combining an adaptive algorithm with a neural network, an adaptive neural network prediction model is established. A numerical example verifies the effectiveness and applicability of the proposed photovoltaic power prediction model [25]. A conceptual model to make a prediction of the PV installed power in Italy through the use of artificial neural networks is developed. This model is also applied to analysis of the spread of this technology in some other European countries [26]. A mathematical model with 7 parameters is represented with a developed MATLAB-Simulink model. All calculations associated to process the genetic algorithms are integrated into one program, with very good convergence. The approach is based on formulating the parameter extraction as a search and optimization problem. Current-voltage

data used were generated by simulating a two-diode solar cell model of specified parameters [27]. The results of performance optimization of a PV/T system with natural air flow operation are presented. A theoretical model is developed and validated with a good agreement between the predicted results and measured data. A genetic algorithm method was applied to find the optimum values of geometric characteristics of the studied PV/T system to achieve higher thermal and electrical efficiencies [28]. A model of a photovoltaic array based on the Radial basis function neural network to decrease the complexity of the modeling is set up in which the solar radiation and ambient temperature impacting on the photovoltaic array are input variables and the output voltage and current corresponding to the maximum power output of photovoltaic array are output variables [29]. An improved modeling technique for a photovoltaic (PV) module, utilizing the optimization ability of a genetic algorithm, is detailed for different parameters computed via this approach. The global optimization of the parameters and the applicability for the entire range of solar radiation and a wide range of temperatures are achievable via this approach. The Manufacturer's data sheet information is used as a basis for parameter optimization, with an average absolute error fitness function formulated, and a numerical iterative method used to solve the voltage-current relation of the PV module [30]. The performance of the Photovoltaic module using a dynamic thermal model is evaluated. Electric circuit elements are used in the proposed dynamic model of the Photovoltaic module. Therefore, the 'Node Analysis' method is used to analyze the nonlinear circuit [31]. The problem of designing an accurate and computationally fast model of a particular real photovoltaic module is introduced. There are a number of well-known theoretical models, but they need the fine tuning of several parameters, whose values are often difficult to estimate. An accurate ANN model of a real ATERSA A55 photovoltaic module is derived [32].

Many benefits drawn from previous works were applied to this work. Global modeling is done by using irradiance and temperature to adapt this module model to a variety of conditions. The results obtained are sufficiently accurate to apply the models to control the PV systems for tracking optimal

power points. The proposed PV-panel model based on ANN and GA can be used to evaluate the performance of the PV-panel using environmental factors and involves less computational efforts. It can also be used for predicting the output electrical energy from the PV-panel. The calculations in this paper are based on practical PV module data in reference [33]. This work addresses the following: Specific and general PV module modeling based on a real panel with the aid of electric circuits with a diode exponential model as a model with moderate complexity and Back-Propagation (BP)) Artificial Neural Network (ANN) techniques due to its advantages. The I-V characteristics equation is solved using Newton's method for rapid convergence of the answer, because the solution of the current is recursive by the inclusion of a series resistance in the model. The first model is validated by comparison of real data from the manufacturer and simulated corresponding data; however the ANN model is validated by comparisons for P-V curves, and excellent acceptable error between targets and outputs. A set of 3D figures (ANN training data) are presented to cover most probable situations at various levels of irradiance and temperature with the current, voltage, and power (i.e. model inputs & outputs). A Genetic Algorithm (GA) is used as an optimization powerful tool to find MPPs over the most probable range. The implemented genetic function efficiently picks the peaks of PV power curves as the objective function and two variables as arguments  $x(1)$ , and  $x(2)$  ( $V_{mp}$ , and  $I_{mp}$ ) with the nonlinear constraints and variables boundaries. A set of 3D figures generated from the genetic function is presented to cover various irradiance, various temperature with optimum current, and optimum voltage at maximum power. An ANN model with back-propagation is adopted using previous 3D graphs as learning data for input and desired target. This model is checked and verified by comparing actual and predicted ANN values, and good error values for shown outputs imply accuracy with an excellent regression factor of 0.99999. The maximum power point identification function using a genetic algorithm and neural network is deduced, to generate the reference values to drive the tracking system in the PV system at optimum operation. The ANN models' algebraic equations are deduced for use directly with their GUI

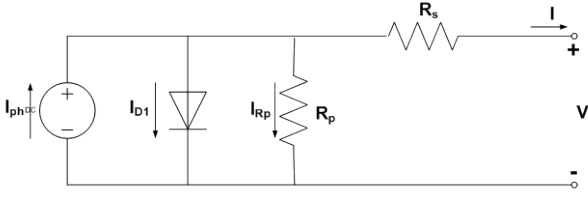


Figure 1: Single exponential model of a PV Cell

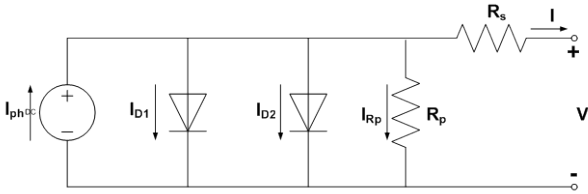


Figure 2: Double exponential model of PV Cell

(Graphical User Interface) blocks and are presented too.

## 2. PV Cell Model

The use of equivalent electric circuits makes it possible to model the characteristics of a PV cell. The method used here is implemented in MATLAB programs for simulations. The same modeling technique is also applicable for modeling a PV module. There are two key parameters frequently used to characterize a PV cell. Shorting together the terminals of the cell, the photon generated current will flow out of the cell as a short-circuit current ( $I_{sc}$ ). Thus,  $I_{ph} = I_{sc}$ , when there is no connection to the PV cell (open-circuit), the photon generated current is shunted internally by the intrinsic p-n junction diode. This gives the open circuit voltage ( $V_{oc}$ ). The PV module or cell manufacturers usually provide the values of these parameters in their datasheets [33]. The ASE-300-DGF/50 is an industrial-grade solar power module built to the highest standards. Extremely powerful and reliable, the module delivers maximum performance in large systems that require higher voltages, including the most challenging conditions of military, utility and commercial installations. For superior performance, quality and peace of mind, the ASE-300-DGF/50 is renowned as the first choice among those who recognize that not all solar modules are created equal [33]. The simplest model of a PV cell equivalent circuit consists of an ideal cur-

rent source in parallel with an ideal diode. The current source represents the current generated by photons (often denoted as  $I_{ph}$  or  $I_L$ ), and its output is constant under constant temperature and constant incident radiation of light. The PV panel is usually represented by the single exponential model or the double exponential model. The single exponential model is shown in Fig. 1. The current is expressed in terms of voltage, current and temperature, as shown in equation (1) [34]. However, equation (2) describes the current in terms of the same parameters for the double exponential model, as shown in Fig. 2 [34].

$$I = I_{ph} - I_o \left\{ \exp \left[ \frac{q(V + IR_s)}{AkT} \right] - 1 \right\} - \frac{V + IR_s}{R_p} \quad (1)$$

$$I = I_{ph} - I_{s1} \left\{ \exp \left[ \frac{q(V + IR_s)}{AkT} \right] - 1 \right\} - I_{s2} \left\{ \exp \left[ \frac{q(V + IR_s)}{AkT} \right] - 1 \right\} - \frac{V + IR_s}{R_p} \quad (2)$$

where:  $I_{ph}$ —the photo generated current,  $I_o$ —the dark saturation current,  $I_{s1}$ —saturation current due to diffusion,  $I_{s2}$ —the saturation current due to recombination in the space charge layer,  $I_{Rp}$ —current flowing in the shunt resistance,  $R_s$ —cell series resistance,  $R_p$ —the cell (shunt) resistance,  $A$ —the diode quality factor,  $q$ —the electronic charge ( $1.6 \times 10^{-19}$  C),  $k$ —the Boltzmann constant ( $1.38 \times 10^{-23}$  J/K) and  $T$ —the ambient temperature in Kelvin.

Eq. (1) and Eq. (2) are both nonlinear. Furthermore, the parameters ( $I_{ph}$ ,  $I_{s1}$ ,  $I_{s2}$ ,  $R_s$ ,  $R_{sh}$  and  $A$ ) vary with temperature, irradiance and depend on manufacturing tolerance. Numerical methods and curve fitting can be used to make estimates [34, 35].

There are three key operating points on the I-V curve of a photovoltaic cell: the short circuit point, maximum power point and the open circuit point. At the open circuit point on the I-V curve,  $V = V_{oc}$  and  $I = 0$ . After substituting these values in the single exponential equation (1) the equation can be obtained [34].

$$0 = I_{ph} - I_o \left\{ \exp \left[ \frac{qV_{oc}}{AkT} \right] - 1 \right\} - \frac{V_{oc}}{R_p} \quad (3)$$

At the short circuit point on the I-V curve,  $I = I_{sc}$  and  $V = 0$ . Similarly, using equation (1), we can obtain.

$$I_{sc} = I_{ph} - I_o \left\{ \exp \left[ \frac{qI_{sc}R_s}{AkT} \right] - 1 \right\} - \frac{I_{sc}R_s}{R_p} \quad (4)$$

At the maximum power point of the I-V curve, we have  $I = I_{mpp}$  and  $V = V_{mpp}$ . We can use these values to obtain the following:

$$I_{mpp} = I_{ph} - I_o \left\{ \exp \left[ \frac{q(V_{mpp} + I_{mpp}R_s)}{AkT} \right] - 1 \right\} - \frac{V_{mpp} + I_{mpp}R_s}{R_p} \quad (5)$$

Power transferred to the load is expressed as

$$P = I \cdot V \quad (6)$$

The diode quality factor could be estimated as [34, 36]:

$$A = \frac{V_{mpp} + I_{mpp}R_{so} - V_{oc}}{V_T \left\{ \ln \left( I_{sc} - \frac{V_{mpp}}{R_{sho}} - I_{mpp} \right) - \ln \left( I_{sc} - \frac{V_{oc}}{R_o} \right) + \frac{I_{mpp}}{I_{sc} - \frac{V_{oc}}{R_{so}}} \right\}} \quad (7)$$

and [34, 36]

$$R_p = R_{sho} \quad (8)$$

$$I_o = \left( I_{sc} - \frac{V_{oc}}{R_p} \right) \exp \left( -\frac{V_{oc}}{AV_T} \right) \quad (9)$$

$$R_s = R_{so} - \frac{AV_T}{I_o} \exp \left( -\frac{V_{oc}}{AV_T} \right) \quad (10)$$

$$I_{ph} = I_{sc} \left( 1 + \frac{R_s}{R_p} \right) + I_o \left( \exp \frac{I_{sc}R_s}{AV_T} - 1 \right) \quad (11)$$

As a very good approximation, the photon generated current, which is equal to  $I_{sc}$ , is directly proportional to the irradiance, the intensity of illumination, to PV cell [37]. Thus, if the value,  $I_{sc}$ , is known from the datasheet, under the standard test condition,  $G_o = 1000 \text{ W/m}^2$  at the air mass ( $AM$ ) = 1.5, then the photon generated current at any other irradiance,  $G$  ( $\text{W/m}^2$ ), is given by:

$$I_{sc|G} = \left( \frac{G}{G_o} \right) I_{sc|G_o} \quad (12)$$

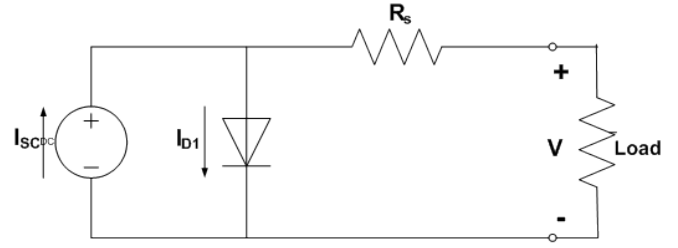


Figure 3: Equivalent circuit used in the simulations

It should be noted that, in a practical PV cell, there is a series of resistance in a current path through the semiconductor material, the metal grid, contacts, and current collecting bus [38]. These resistive losses are lumped together as a series resistor ( $R_s$ ). Its effect becomes very conspicuous in a PV module that consists of many series-connected cells, and the value of resistance is multiplied by the number of cells. Shunt resistance is a loss associated with a small leakage of current through a resistive path in parallel with the intrinsic device [38]. This can be represented by a parallel resistor ( $R_p$ ). Since its effect is much less conspicuous in a PV module compared to the series resistance, it may be ignored [38], [39].

### 3. Photovoltaic Module Modeling

A single PV cell produces an output voltage less than 1 V, thus a number of PV cells are connected in series to achieve a desired output voltage. When series-connected cells are placed in a frame, it is called as a module. When the PV cells are wired together in series, the current output is the same as the single cell, but the voltage output is the sum of each cell voltage. Also, multiple modules can be wired together in series or parallel to deliver the voltage and current level needed. The group of modules is called an array. The panel construction provides protection for individual cells from water, dust etc., as the solar cells are placed in an encapsulation of flat glass. Our case here depicts a typical connection of 216 cells that are connected in series [33]. The strategy of modeling a PV module is no different from modeling a PV cell. It uses the same PV cell model. The parameters are all the same; only the voltage parameter (such as the open-circuit voltage) is different and must be divided by the number of cells. An electric model with moderate complexity [40] is

shown in figure 3, and provides fairly accurate results. The model consists of a current source ( $I_{sc}$ ), a diode ( $D$ ), and series resistance ( $R_s$ ). The effect of parallel resistance ( $R_p$ ) is very small in a single module, thus the model does not include it. To make a better model, it also includes temperature effects on the short-circuit current ( $I_{sc}$ ) and the reverse saturation current of diode ( $I_o$ ). It uses a single diode, with the diode ideality factor set to achieve the best I-V curve match.

Equation (13) describes the current-voltage relationship of the PV cell.

$$I = I_{sc} - I_o \left( \exp \left( q \left( \frac{V + IR_s}{AkT} \right) \right) - 1 \right) \quad (13)$$

Where:  $I$  is the cell current (the same as the module current),  $V$  is the cell voltage = {module voltage} ÷ {No. of cells in series},  $T$  is the cell temperature in Kelvin (K).

First, calculate the short-circuit current ( $I_{sc}$ ) at a given cell temperature ( $T$ ):

$$I_{sc|T} = I_{sc|T_{ref}} \left[ 1 + a(T - T_{ref}) \right] \quad (14)$$

Where:  $I_{sc}$  at  $T_{ref}$  is given in the datasheet (measured under irradiance of 1000 W/m<sup>2</sup>),  $T_{ref}$  is the reference temperature of PV cell in Kelvin (K), usually 298 K (25°C),  $a$  is the temperature coefficient of  $I_{sc}$  in percent change per degree temperature also given in the datasheet.

The short-circuit current ( $I_{sc}$ ) is proportional to the intensity of irradiance, thus  $I_{sc}$  at a given irradiance ( $G$ ) is introduced by Eq. (12).

The reverse saturation current of diode ( $I_o$ ) at the reference temperature ( $T_{ref}$ ) is given by Eq. (15) with the diode ideality factor added:

$$I_o = \frac{I_{sc}}{\exp \left( \frac{qV_{oc}}{AkT} \right) - 1} \quad (15)$$

The reverse saturation current ( $I_o$ ) is temperature dependant and  $I_o$  at a given temperature ( $T$ ) is calculated using the following equation [40].

$$I_{o|T} = I_{o|T_{ref}} \left( \frac{T}{T_{ref}} \right)^{\frac{3}{A}} \exp \left( \frac{-qE_g}{Ak} \left( \frac{1}{T} - \frac{1}{T_{ref}} \right) \right) \quad (16)$$

The diode ideality factor ( $A$ ) takes a value between one and two; however, a more accurate value is estimated by curve fitting [40]. It can also be estimated by trial and error until an accurate value is achieved.  $E_g$  is the Band gap energy (1.12 V (Si); 1.42 (GaAs); 1.5 (CdTe); 1.75 (amorphous Si)).

The series resistance ( $R_s$ ) of the PV module has a large impact on the slope of the I-V curve near the open-circuit voltage ( $V_{oc}$ ), hence the value of  $R_s$  is calculated by evaluating the slope  $dI/dV$  of the I-V curve at the  $V_{oc}$  [40]. The equation for  $R_s$  is derived by differentiating the I-V equation and then rearranging it in terms of  $R_s$  as introduced in equation (17).

$$R_s = - \frac{dV}{dI} \Big|_{V_{oc}} - \frac{AkT/q}{I_o \exp \left( \frac{qV_{oc}}{AkT} \right)} \quad (17)$$

Where:  $\frac{dV}{dI} \Big|_{V_{oc}}$  is the slope of the I-V curve at the  $V_{oc}$  (using the I-V curve in the datasheet then divide it by the number of cells in series);  $V_{oc}$  is the open-circuit voltage of the cell (dividing  $V_{oc}$  in the datasheet by the number of cells in series).

Finally, the equation of I-V characteristics is solved using Newton's method for rapid convergence of the answer, because the solution of current is recursive by the inclusion of a series resistance in the model [40]. Newton's method is described as:

$$x_{n+1} = x_n - \frac{f(x_n)}{f'(x_n)} \quad (18)$$

Where:  $f'(x_n)$  is the derivative of the function,  $f(x) = 0$ ,  $x_n$  is a present value, and  $x_{n+1}$  is a next value.

$$f(I) = I_{sc} - I - I_o \left( \exp \left( q \left( \frac{V + IR_s}{AkT} \right) \right) - 1 \right) = 0 \quad (19)$$

By using the above equations the following output current ( $I$ ) is computed iteratively.

$$I_{n+1} = I_n - \frac{I_{sc} - I_n - I_o \left( \exp \left( q \left( \frac{V + I_n R_s}{AkT} \right) \right) - 1 \right)}{-1 - I_o \left( \frac{qR_s}{AkT} \right) \exp \left( q \left( \frac{V + I_n R_s}{AkT} \right) \right)} \quad (20)$$

Fig. 4 presents a comparison between real data from the manufacturer [33], data sheet (Red cubic), with simulated data with blue lines. Simply, these curves

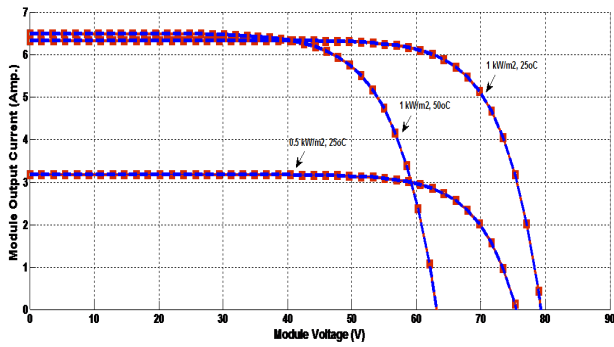


Figure 4: Real and theoretical comparisons



Figure 7: I-V curves (0.50 kW/m<sup>2</sup>; 0, 25, 50, 75°C)

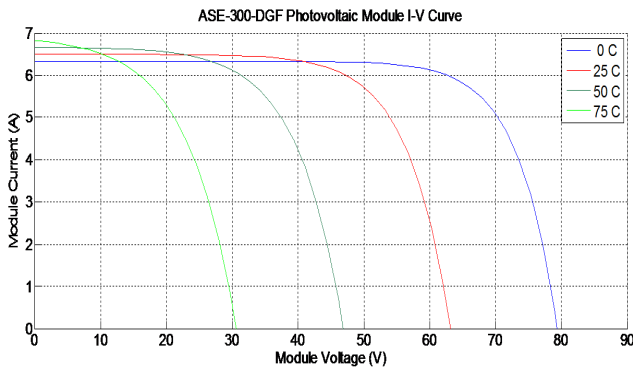


Figure 5: I-V curves at (1 kW/m<sup>2</sup>; 0, 25, 50, 75°C)

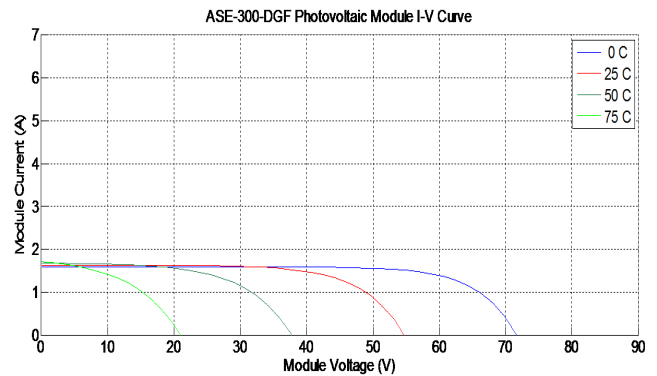


Figure 8: I-V curves (0.25 kW/m<sup>2</sup>; 0, 25, 50, 75°C)

show a great match between real and theoretical data to validate it.

The figures of I-V characteristics at various module temperatures are simulated with the MATLAB model for our PV module and shown in figures from Fig. 5 to Fig. 8.

Then, a set of 3D figures (from Fig. 9 to Fig. 20) are proposed to cover the most probable situations at various irradiance, various temperature with the current, the voltage, and the power. These surface face rela-

tions will be considered later, as learning or training data for the general neural network simulation.

The neural network has the ability to deal with all previous relations as a surface or mapping face, due to its technical ability to interpolate in-between points and curves. At a later stage a more powerful tool is used (Genetic Algorithm) to find MPPs over the most probable range.

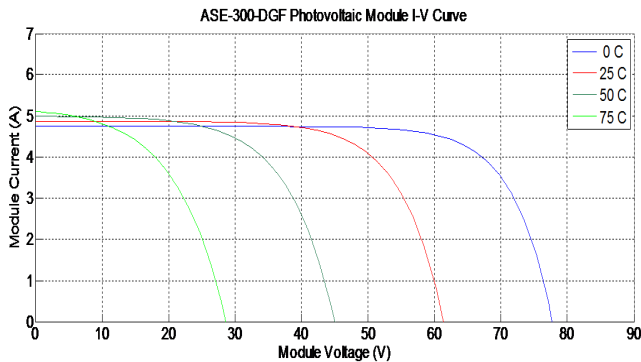


Figure 6: I-V curves (0.75 kW/m<sup>2</sup>; 0, 25, 50, 75°C)

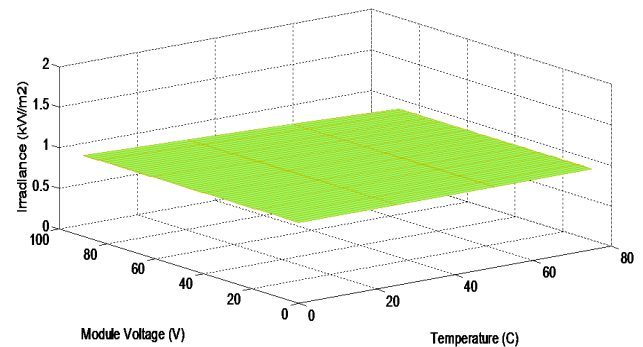


Figure 9: Voltage & Temp. & (1 kW/m<sup>2</sup>) Irradiance

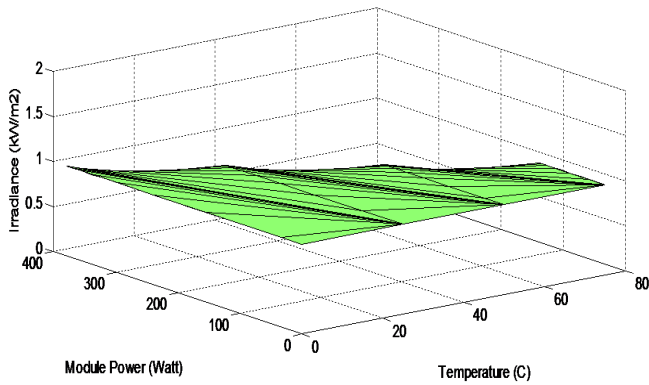


Figure 10: Power & Temp. & (1 kW/m<sup>2</sup>) Irradiance

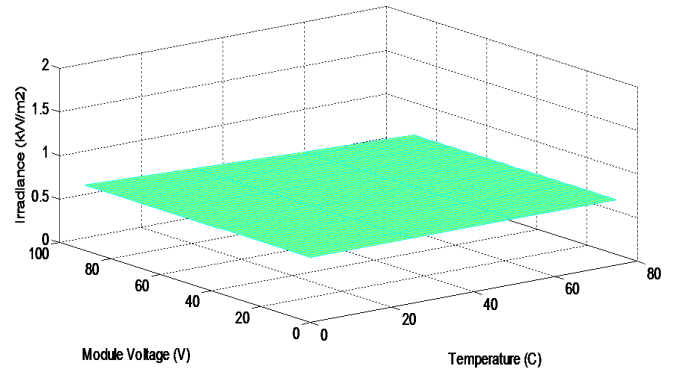


Figure 12: Voltage & Temperature & (0.75 kW/m<sup>2</sup>)

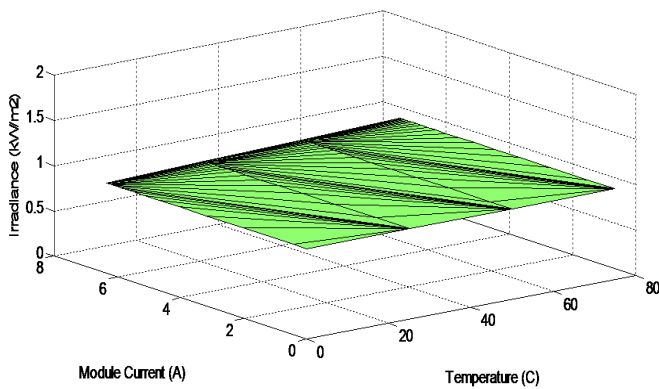


Figure 11: Current & Temp. & (1 kW/m<sup>2</sup>) Irradiance

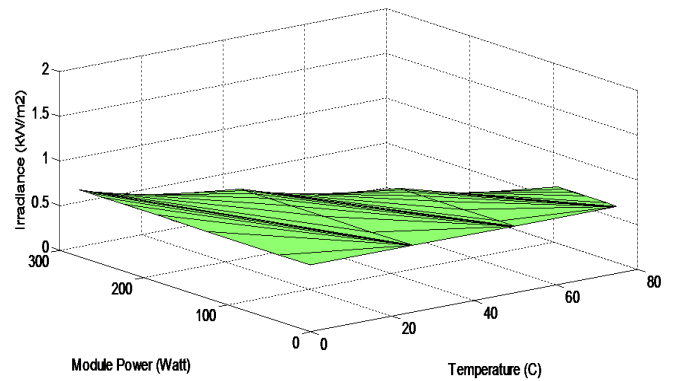


Figure 13: Power & Temperature & (0.75 kW/m<sup>2</sup>)

#### 4. ANN PV Module Model

This model uses the ANN technique, which was used and verified before in many fields [11–15, 41–47]. This model uses the previous 3D graphs illustrated before as training or learning data for input and desired target. The inputs in this model are Irradiance and Temperature; the outputs are: Module Voltage, Current, and Power. This model with its hidden and output layers' suitable neurons number is depicted in Fig. 21. Also, the training state and neural network model in GUI are presented in Fig. 22 and 23 respectively.

P-V relations comparisons (lines and brown cubes) between actual and predicted values at various module temperatures and irradiance are presented in Fig. 24 to Fig. 27. It is shown as a great match between them, with very little error. It is clear there is a unique point for every case at which the maximum power arises.

Fig. 28 and Fig. 29 show the errors for current and

voltage respectively. It is clear the errors for both imply to good results and excellent match for the variables. The error for both is within 2e-7.

The normalized inputs  $G_n$ : (Normalized Irradiance);  $T_n$ : (Normalized Temperature) are as follows:

$$G_n = (G - 0.6250) / 0.2797 \quad (21)$$

$$T_n = (T - 37.5000) / 27.9683 \quad (22)$$

Equations (21) and (22) present the normalized inputs for irradiance and temperature, also the following equations lead to the required derived outputs equations.

$$E1 = -0.3884G_n - 0.8968T_n + 2.8411 \quad (23)$$

$$F1 = 1 / (1 + \exp(-E1))$$

$$E2 = 10.8335G_n - 0.1120T_n - 4.7062 \quad (24)$$

$$F2 = 1 / (1 + \exp(-E2))$$

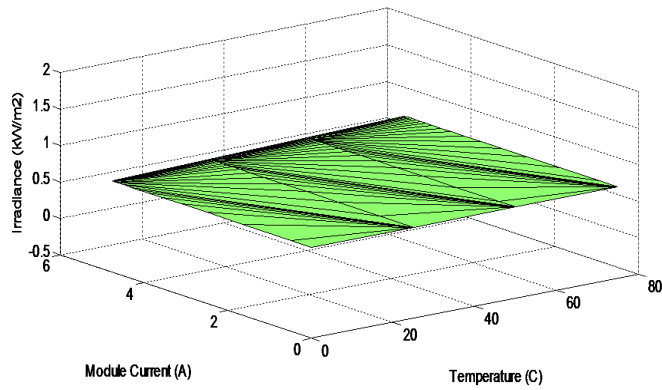


Figure 14: Current & Temperature & (0.75 kW/m<sup>2</sup>)

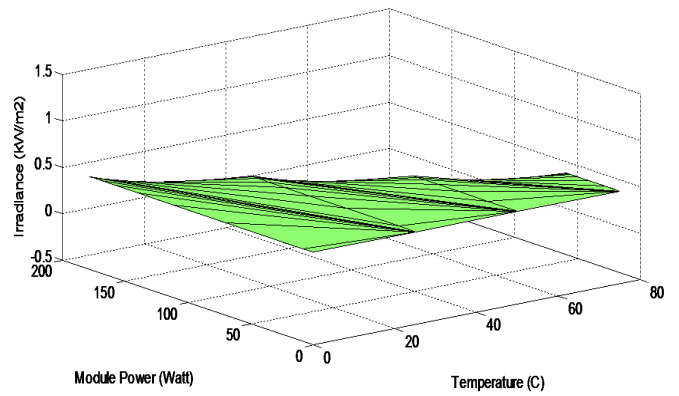


Figure 16: Power & Temperature & (0.50 kW/m<sup>2</sup>)

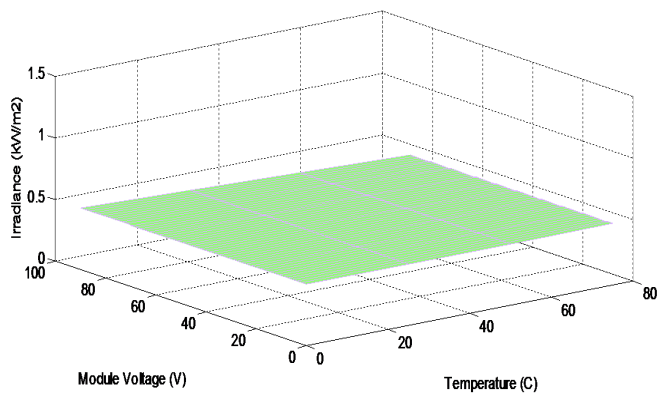


Figure 15: Voltage & Temperature & (0.50 kW/m<sup>2</sup>)

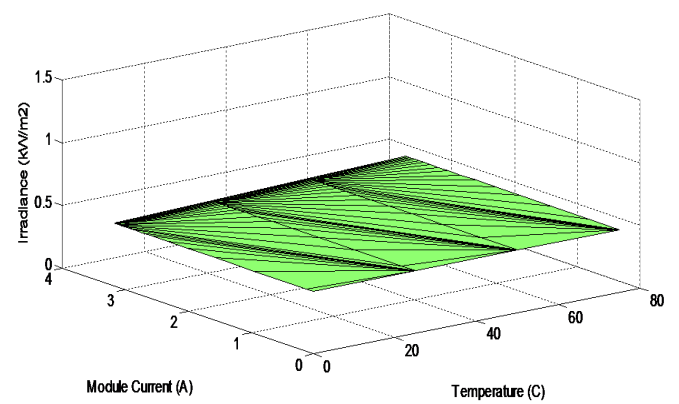


Figure 17: Current & Temperature & (0.50 kW/m<sup>2</sup>)

$$\begin{aligned} E3 &= -0.3773G_n - 9.6071T_n + 7.2495 \\ F3 &= 1/(1 + \exp(-E3)) \end{aligned} \quad (25)$$

$$\begin{aligned} E8 &= 11.6503G_n - 1.1094T_n + 11.1433 \\ F8 &= 1/(1 + \exp(-E8)) \end{aligned} \quad (30)$$

$$\begin{aligned} E4 &= -0.0696G_n - 9.4705T_n - 5.0369 \\ F4 &= 1/(1 + \exp(-E4)) \end{aligned} \quad (26)$$

$$\begin{aligned} E9 &= 0.2372G_n - 0.8735T_n + 0.7613 \\ F9 &= 1/(1 + \exp(-E9)) \end{aligned} \quad (31)$$

The normalized outputs are:

$$\begin{aligned} E5 &= 6.3252G_n + 0.3523T_n + 4.6963 \\ F5 &= 1/(1 + \exp(-E5)) \end{aligned} \quad (27)$$

$$\begin{aligned} V_n &= 0.0466F1 + 0.0080F2 + 0.0661F3 - 0.2311F4 \\ &\quad - 0.0071F5 + 2.5608F6 + 0.0771F7 + 0.0091F8 \\ &\quad - 0.0217F9 - 2.7656 \end{aligned} \quad (32)$$

$$\begin{aligned} E6 &= -0.1062G_n + 3.4660T_n + 8.7149 \\ F6 &= 1/(1 + \exp(-E6)) \end{aligned} \quad (28)$$

$$\begin{aligned} I_n &= 6.2907F1 + 1.5501F2 + 0.2881F3 + 1.8330F4 \\ &\quad - 1.1986F5 - 0.6123F6 - 1.2526F7 + 1.6547F8 \\ &\quad - 2.6831F9 - 6.1682 \end{aligned} \quad (33)$$

$$\begin{aligned} E7 &= 0.1802G_n + 4.0327T_n + 3.7157 \\ F7 &= 1/(1 + \exp(-E7)) \end{aligned} \quad (29)$$

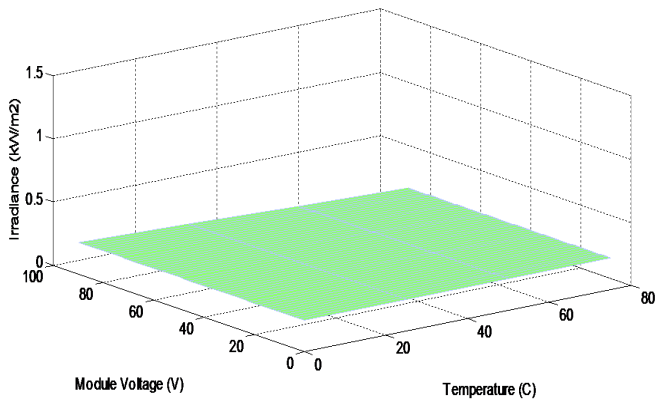


Figure 18: Voltage & Temperature & (0.25 kW/m<sup>2</sup>)

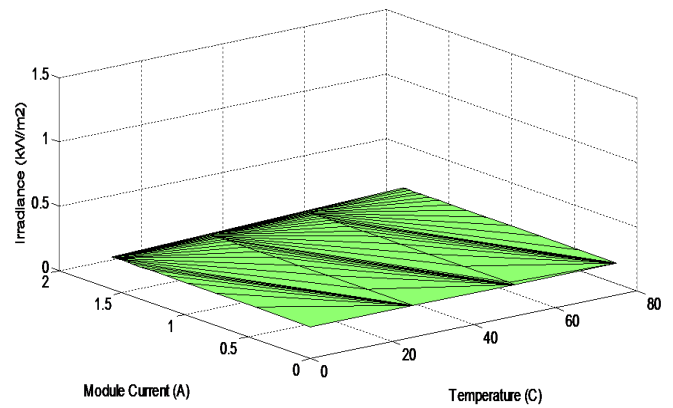


Figure 20: Current & Temperature & (0.25 kW/m<sup>2</sup>)

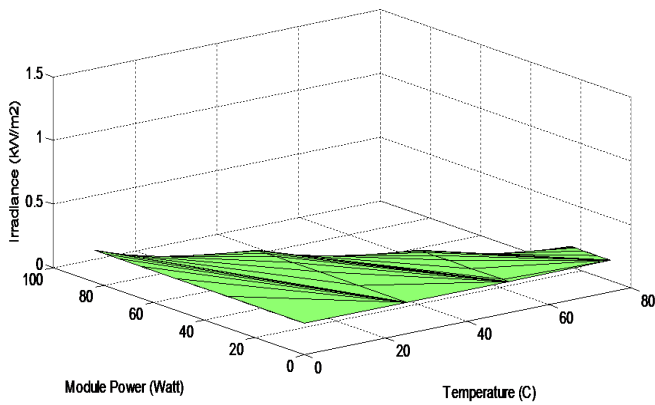


Figure 19: Power & Temperature & (0.25 kW/m<sup>2</sup>)

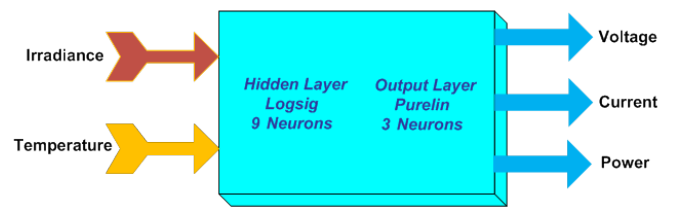


Figure 21: ANN PV Cell Module Model

they connect all the desired input and output parameters as illustrated before for this model.

$$P_n = 7.2249F1 + 1.7820F2 + 1.0262F3 + 5.1377F4 - 1.3507F5 - 0.9574F6 + 3.4515F7 + 1.8830F8 - 6.9036F9 - 7.3615 \quad (34)$$

The unnormalized outputs

$$V = 25.2226V_n + 42.6563 \quad (35)$$

$$I = 2.1788I_n + 2.318 \quad (36)$$

$$P = 57.5303P_n + 81.4030 \quad (37)$$

The ANN model for the PV module is expressed in the form of algebraic equations from Eq. (21) to Eq. (37), which are considered to be the result of the work. These equations could be used directly without training the neural network every time; moreover

## 5. Genetic Algorithm

The genetic algorithm is a method for solving both constrained and unconstrained optimization problems that is based on natural selection, the process that drives biological evolution. The genetic algorithm repeatedly modifies a population of individual solutions. At each step, the genetic algorithm selects individuals at random from the current population to be parents and uses them to produce the children for the next generation. Over successive generations, the population "evolves" toward an optimal solution. We can apply the genetic algorithm to solve a variety of optimization problems that are not well suited for standard optimization algorithms, including problems in which the objective function is discontinuous, non-differentiable, stochastic, or highly nonlinear [48–53].

The genetic algorithm uses three main types of rules at each step to create the next generation from the current population:

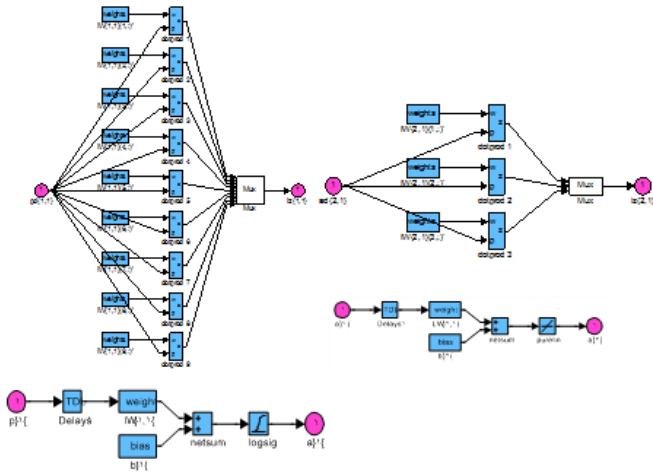


Figure 22: ANN Model with its layers, neurons and weights

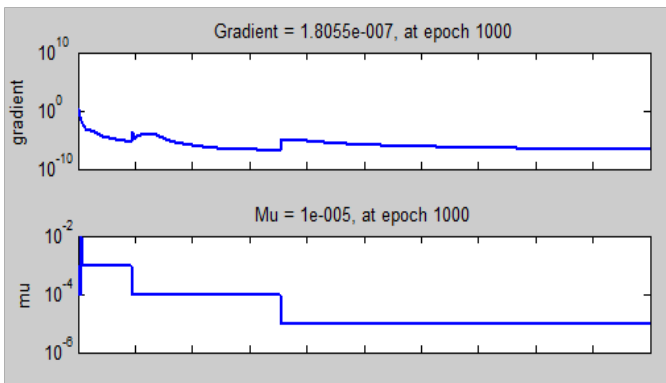


Figure 23: Training State

- Selection rules select the individuals, called parents, which contribute to the population at the next generation.
- Crossover rules combine two parents to form children for the next generation.
- Mutation rules apply random changes to individual parents to form children.

Our genetic trial uses the following MATLAB prescribed terminologies:

Population type: Double Vector with Populations size = 20; Creation function, Initial population, Initial Score, and Initial range: Default; Fitness scaling: Rank; Selection function: Stochastic uniform Reproduction; Elite Count: Default (3), Crossover fraction: Default (0.8); Mutation function: Adaptive feasible (due to its benefits); Crossover function: Scattered Migration; Direction: Forward, Fraction:

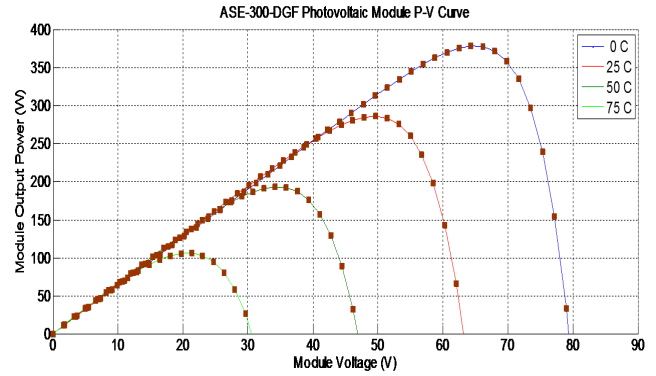


Figure 24: P-V curves at (1 kW/m<sup>2</sup>; 0, 25, 50, 75°C)

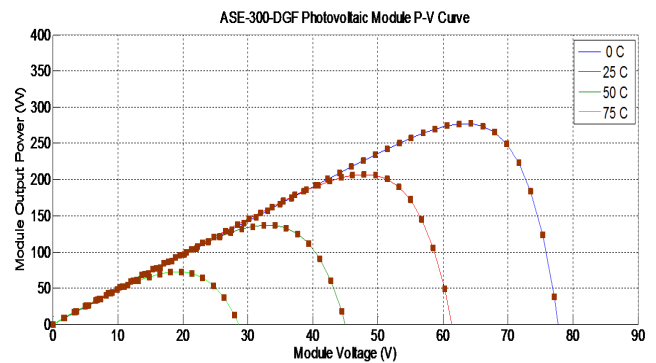


Figure 25: P-V curves (0.75 kW/m<sup>2</sup>; 0, 25, 50, 75°C)

Default (0.2), Interval: Default (20); Stopping criteria (Defaults): Generations: 100, Time limit: Inf., Fitness limit: Inf., Stall generations: 50, Stall time limit: Inf., Function Tolerance: 1e-6, nonlinear constraint tolerance: 1e-6. Also, this technique was used previously by the same authors in the field of green energy in [11, 12, 27, 28, 54–56].

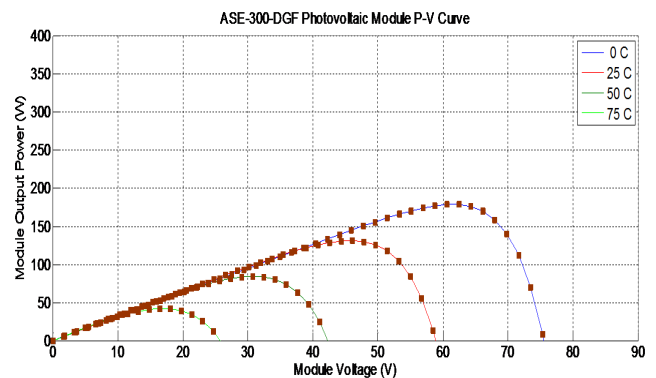


Figure 26: P-V curves (0.50 kW/m<sup>2</sup>; 0, 25, 50, 75°C)

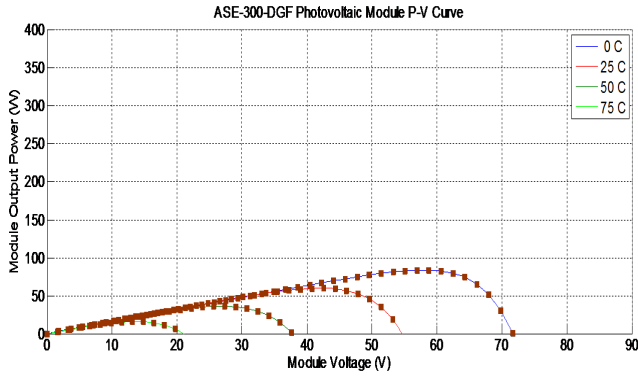


Figure 27: P-V curves (0.25 kW/m<sup>2</sup>; 0, 25, 50, 75°C)

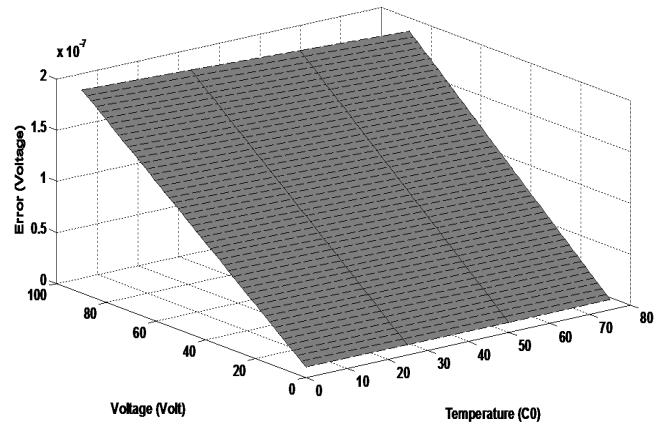


Figure 29: Voltage Error w.r.t. temperature and voltage value

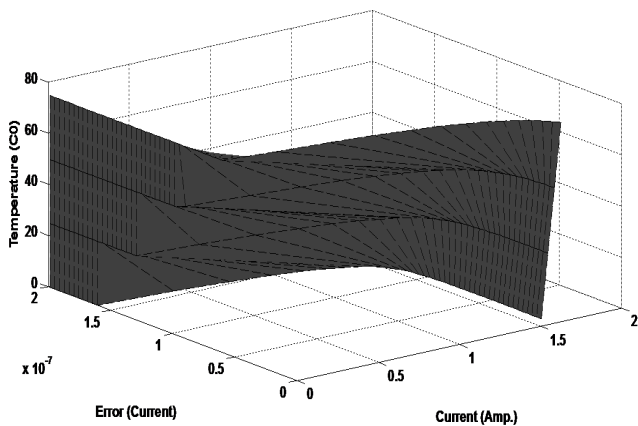


Figure 28: Current Error w.r.t. temperature and current value

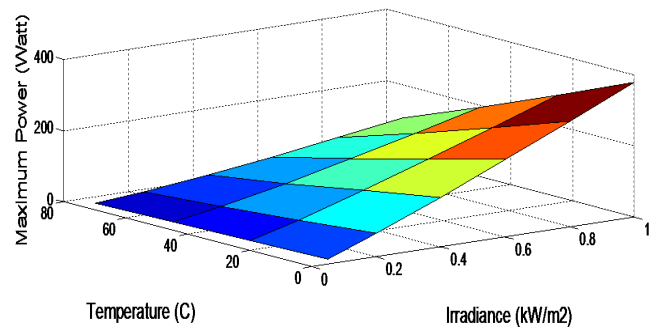


Figure 30: Maximum Power relation with Irradiance and Temperature

### 5.1. Maximum Power GA Function

The aim of this function is to pick the peaks of PV power curves, shown before, as the objective function and two variables as arguments  $x(1)$ , and  $x(2)$  ( $V_{mp}$  and  $I_{mp}$ ).

This efficient function is implemented by maximizing the power with the voltage and current as optimizing variables, and with boundaries for them by the values of  $V_{oc}$ , and  $I_{sc}$  from the PV module data sheet, also with nonlinear constraints with the aid of  $V_{oc}$ , and  $I_{sc}$  obtained from I-V curves for all irradiance and temperature values. Both the objective function and constraint function are implemented using the previous modeling relations in the form of MATLAB m-files.

Function  $MPP = f(x)$

$$MPP = x(1) \cdot x(2) \quad (38)$$

Function Constraints:

This optimizing variable ( $x(1)$ ) is bounded by  $[0 V_{ocDataSheet}]$ .

This optimizing variable ( $x(2)$ ) is bounded by  $[0 I_{scDataSheet}]$ .

The nonlinear constraint:

Function  $[c, ceq] = f(x)$

$$c = [z1 - V_{oc Module(For Every Irradiance \& Temperature Value)}; z2 - I_{sc Module(For Every Irradiance \& Temperature Value)}] \\ ceq = [] \quad (39)$$

The previous equations for constraints (39), imply that,  $c$ —limits the voltage and current by open circuit voltage and short circuit current at every irradiance and temperature value and  $ceq$ —for the equality constraints and there are no equality constraints for our case so it remains empty in the code  $[]$ .

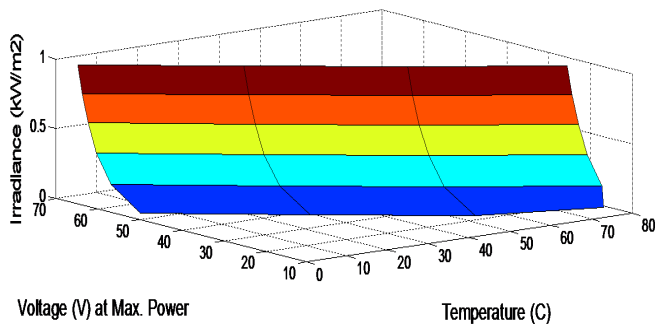


Figure 31: Voltage at Maximum Power relation with Irradiance and Temperature

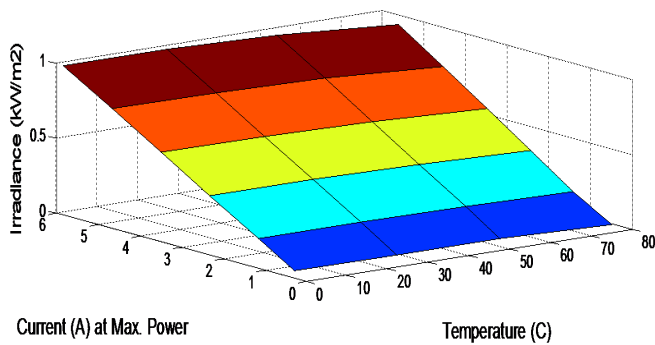


Figure 32: Current at Maximum Power relation with Irradiance and Temperature

### 5.2. Genetic Algorithm Results

Finally, a set of 3D figures are proposed to cover the most probable situations at various irradiance and temperature values with the current, the voltage, and the power at the desired maximum power. The figures from Fig. 30 to Fig 32 result from the optimum genetic function implemented previously to give the required driving parameters for the PV sun tracker system to work at optimum performance. These surface face relations will be considered later as learning or training data for the ANN model. The following figures cover the most probable range for both irradiance (0.05:1 kW/m<sup>2</sup>) and temperature (0:75°C).

The neural network has the ability to deal with all previous relations as a surface or mapping face, due to its technical ability to interpolate in-between points and curves.

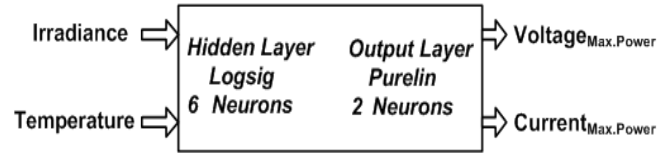


Figure 33: ANN Optimum PV Module Model

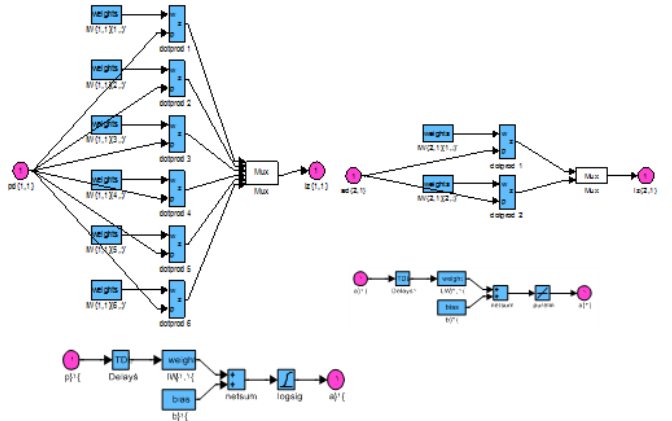


Figure 34: ANN Model with its layers, neurons, and weights

## 6. ANN PV GA Function with its regression function

This model uses ANN with back-propagation which was previously used, described and verified in the field of renewable energy such as in [11–15, 41–47]. This model uses the 3D graphs (Fig. 30 to Fig. 32) illustrated before as training or learning data for input and desired target. The inputs in this model are Irradiance and Temperature; the outputs are: Module Voltage, and Current at maximum Power. This model with its hidden and output layers' suitable neuron numbers is depicted in Fig. 33. A neural net-

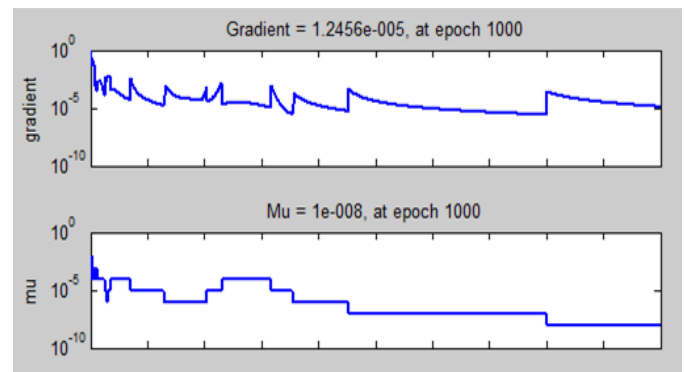


Figure 35: Training State

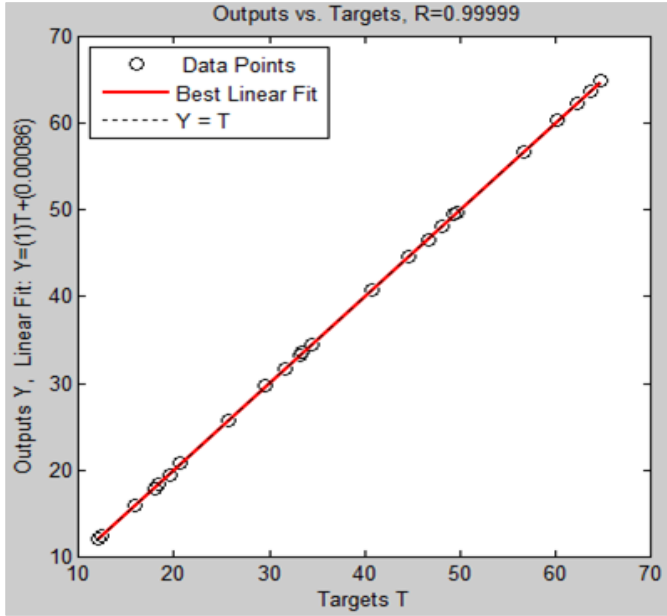


Figure 36: Comparisons of actual and ANN-predicted values for Voltage

work model in GUI with its structure, layers, neurons and weights is presented in Fig. 34. The training state and comparisons check are introduced in Figs. 35, and 36 respectively.

Fig. 37 and Fig. 38 show the errors for current and voltage respectively. It is clear the errors for both imply good results and an excellent match for the variables. The error for both lies within  $1e-8$ .

The regression neural network function is deduced as follows:

The normalized inputs  $G_n$ : (Normalized Irradiance);

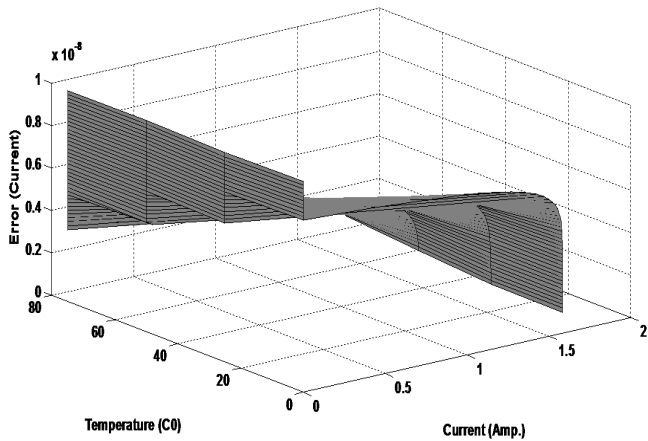


Figure 37: Optimum Current Error w.r.t. temp. and current

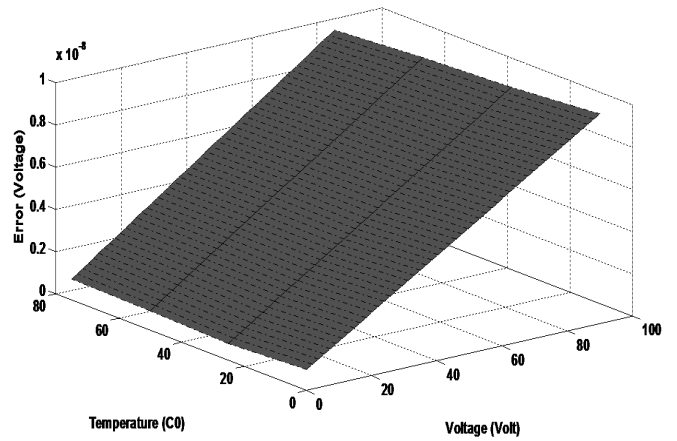


Figure 38: Optimum Voltage Error w.r.t. temp. and voltage

$T_n$ : (Normalized Temperature) are:

$$G_n = (G - 0.5083) / 0.3368 \quad (40)$$

$$T_n = (T - 37.5000) / 28.5520 \quad (41)$$

The following equations lead to the required derived output equations.

$$E1 = 8.8013G_n + 32.6047T_n - 31.3610 \quad (42)$$

$$F1 = 1 / (1 + \exp(-E1))$$

$$E2 = 0.1741G_n - 0.2375T_n - 0.0988 \quad (43)$$

$$F2 = 1 / (1 + \exp(-E2))$$

$$E3 = 0.0580G_n + 6.2039T_n + 1.0561 \quad (44)$$

$$F3 = 1 / (1 + \exp(-E3))$$

$$E4 = -0.0352G_n - 13.9139T_n - 4.7855 \quad (45)$$

$$F4 = 1 / (1 + \exp(-E4))$$

$$E5 = -2.3454G_n + 0.0302T_n - 8.5850 \quad (46)$$

$$F5 = 1 / (1 + \exp(-E5))$$

$$E6 = -0.2908G_n - 16.7000T_n - 19.6496 \quad (47)$$

$$F6 = 1 / (1 + \exp(-E6))$$

The normalized outputs are:

$$V_n = -0.6907F1 + 3.0723F2 + 2.2439F3 + 3.2258F4 - 123.3601F5 + 0.4641F6 - 3.9162 \quad (48)$$

$$I_n = 0.1583F1 + 22.0215F2 + 36.2987F3 + 36.3581F4 + 1.2441F5 - 3.4176F6 - 45.3856 \quad (49)$$

The unnormalized outputs are:

$$V = 17.3087V_n + 37.2067 \quad (50)$$

$$I = 1.9128I_n + 2.7979 \quad (51)$$

The optimum ANN model for PV module is expressed in the form of algebraic equations from Eq. (40) to Eq. (51), which are considered to be the result of the work. These equations could be used directly without training the neural network every time; moreover they connect all the desired inputs and outputs parameters as illustrated before for this model to drive the module into optimum operation.

## 7. Conclusion

Due to the importance of photovoltaic systems especially in the field of green energy, this paper presents a simple but efficient PV modeling trial for both specific and general systems. It models each component and simulates them using MATLAB. The result shows that the PV model using an equivalent circuit in moderate complexity provides good matching with the real PV module. Simulations are based on the Schott ASE-300-DGF PV panel. Non-specific modeling and simulation in more probable situations for variable values of temperature and irradiance are presented. The simulation results at each irradiance value with various temperature values and corresponding characteristics are well depicted in 3D figures. An Artificial Neural Network (ANN) is used for the proposed range of irradiance and temperature as model inputs, with the corresponding values of voltage, current and power as outputs with algebraic equations. Then, it introduces an efficient identification method for the maximum power point

(MPP) function for the PV module using the genetic algorithm (GA). The required function to generate the reference values to drive the tracking system in the PV system at MPP is done with the aid of ANN. This function uses the most probable situations for variable values of temperature and irradiance to obtain the corresponding voltage and current at maximum power. The aim of this paper is to pick peaks of the power curves (maximum points) to make the sun tracker work efficiently. The simulation results at MPP are well depicted in 3D figures, to be used as training or learning data for the ANN model. The ANN regression function for this unit is introduced for use directly, without operating the neural model every time. The neural network units are implemented using the back propagation (BP) learning algorithm, due to its ability to predict values in-between learning values and to make interpolations in-between learning curves data. This is done with a suitable number of network layers and neurons at minimum error and in a precise manner. The numbers of neurons and layers are selected to lend more accuracy to the model with back-propagation—with two layers: one hidden layer and the other output layer. This configuration is considered to be a general approximator to any function with a log-sigmoid function in the hidden layer and pure-line for the output layer. The number of neurons in the output layer has to be the same as the output variables number. The number of neurons in the hidden layer is selected by inspection or by trial and error until one attains the desired performance goal, accuracy, minimum error with little time for training and with as low a number of neurons as possible with the aid of MATLAB and toolbox.

Finally, the results obtained are sufficiently accurate to apply the models for controlling the PV systems for tracking the optimal power points. The proposed PV-panel model based on ANN and GA make it possible to evaluate the performance of the PV-panel using only the environmental factors; it also involves less computational effort and can be used for predicting the output electrical energy from the PV-panel and then conducting operations at optimum performance.

## References

- [1] [s.n.], \Trends in photovoltaic applications. survey report of selected iea countries between 1992 and 2006.
- [2] T. Markvart, L. Castaner, Practical Handbook of Photovoltaics, Fundamentals and Applications, Elsevier, 2003.
- [3] A. El Shahat, Dc-dc converter duty cycle ann estimation for dg applications, *Journal of Electrical Systems* 9 (1) (2013) 13–38.
- [4] A. El Shahat, Photovoltaic power system simulation for micro – grid distribution generation, in: 8th International Conference on Electrical Engineering (ICEENG 2012), Military Technical College, Egypt, 2012.
- [5] A. Chatterjee, A. Keyhani, D. Kapoor, Identification of photovoltaic source models, *IEEE Transactions on Energy Conversion* 26 (3) (2011) 883–889.
- [6] A. Keyhani, Modeling of photovoltaic microgrids for bulk power grid studies, in: IEEE Power & Energy Society General Meeting, Detroit, Michigan, 2011.
- [7] K. Hussein, I. Muta, T. Hoshino, M. Osakada, Maximum photovoltaic power tracking: an algorithm for rapidly changing atmospheric conditions, *Generation, Transmission and Distribution, IEE Proceedings-* 142 (1995) 59–64.
- [8] D. Hohm, M. Ropp, Comparative study of maximum power point tracking algorithms using an experimental, programmable, maximum power point tracking test bed, in: Photovoltaic Specialists Conference, 2000. Conference Record of the Twenty-Eighth IEEE, 2000, pp. 1699–1702.
- [9] D. Sera, R. Teodorescu, P. Rodriguez, Pv panel model based on datasheet values, in: Industrial Electronics, 2007. ISIE 2007. IEEE International Symposium on, 2007, pp. 2392–2396.
- [10] D. P. Hohm, M. E. Ropp, Comparative study of maximum power point tracking algorithms, *Progress in Photovoltaics: Research and Applications* 11 (2003) 47–62.
- [11] S. Premrudeepreechacharn, N. Patanapirom, Solar-array modelling and maximum power point tracking using neural networks, in: IEEE Bologna Power Tech Conference, Bologna, Italy, 2003.
- [12] L. Zhang, Y. F. Bai, Genetic algorithm-trained radial basis function neural networks for modelling photovoltaic panels, *Engineering Applications of Artificial Intelligence Journal* 18 (7) (2005) 833–844.
- [13] H. Mekki, A. Mellit, H. Salhi, K. Belhout, Modeling and simulation of photovoltaic panel based on artificial neural networks and vhdl-language, in: 4th International Conference on Computer Integrated Manufacturing CIP'2007, 2007.
- [14] M. G. Villalva, J. R. Gazoli, E. R. Filho, Comprehensive approach to modeling and simulation of photovoltaic arrays, *Power Electronics, IEEE Transactions on* 24 (5) (2009) 1198–1208.
- [15] S. I. Sulaiman, T. K. Abdul Rahman, I. Musirin, S. Shaari, Optimizing three-layer neural network model for grid-connected photovoltaic system output prediction, in: Innovative Technologies in Intelligent Systems and Industrial Applications (CITISIA 2009), 2009, pp. 338–343.
- [16] F.-M. Petcut, T. Leonida-Dragomir, Solar cell parameter identification using genetic algorithms, *Control Engineering and Applied Informatics* 12 (1) (2010) 30–37.
- [17] D. M. Riley, G. K. Venayagamoorthy, Comparison of a recurrent neural network pv system model with a traditional component – based pv system model, in: 37th IEEE Photovoltaic Specialists Conference, Seattle, WA, USA, 2011.
- [18] S. Hadji, J.-P. Gaubert, F. Krim, Genetic algorithms for maximum power point tracking in photovoltaic systems, in: Proceedings of the 2011-14th European Conference Power Electronics and Applications (EPE 2011), Birmingham, 2011.
- [19] Y. P. Chang, Optimal tilt angle for pv modules using the neural-genetic algorithm considering mathematical model of the solar orbit and position, in: Advanced Materials Research, 2012, pp. 250–253.
- [20] M. Hadjab, S. Berrah, H. Abid, Neural network for modeling solar panel, *International Journal of Energy* 6 (1) (2012) 9–16.
- [21] J. L. Gao, Modeling of photovoltaic cell based on bp neural networks improved by mea, *Applied Mechanics and Materials* 217–219 (2012) 809–814.
- [22] F. Bonanno, G. Capizzi, C. Napoli, G. Graditi, G. M. Tina, A radial basis function neural network based approach for the electrical characteristics estimation of a photovoltaic module, *Applied Energy Journal* 97 (2012) 956–961.
- [23] H. Ravaee, S. Farahat, F. Sarhaddi, Artificial neural network based model of photovoltaic thermal (pv/t) collector, *The Journal of Mathematics and Computer Science* 4 (3) (2012) 411–417.
- [24] J. K. Maherchandani, C. Agarwal, M. Sahi, Estimation of solar cell model parameter by hybrid genetic algorithm using matlab, *International Journal of Advanced Research in Computer Engineering & Technology (IJARCET)* 1 (6) (2012) 78–81.
- [25] D. Niu, Y. Wei, Y. Chen, Photovoltaic power prediction based on scene simulation knowledge mining and adaptive neural network, Hindawi Publishing Corporation, *Mathematical Problems in Engineering Journal*, Article ID 260351 2013 (2013) 6 pages.
- [26] C. Gallo, M. De Bonis, A neural network model for forecasting photovoltaic deployment in italy, *International Journal of Sustainable Energy and Environment* 1 (1) (2013) 1–13.
- [27] G. Venkateswarlu, P. S. Raju, Modeling and parameter extraction of pv modules using genetic algorithms and differential evaluation, *IOSR Journal of Electrical and Electronics Engineering (IOSR-JEEE)* 5 (6) (2013) 37–44.
- [28] A. Shahsavari, P. Talebizadeh, H. Tabaei, Optimization with genetic algorithm of a pv/t air collector with natural air flow and a case study, *Journal of Renewable and Sustainable Energy* 5 (2013) 023118. doi:10.1063/1.4798312.

- [29] N. Ngu, H. Wang, L. Tam, Comparison of radial basis function neural network and back propagation neural network in controller for photovoltaic-array modeling and maximum power point tracking, *Advanced Science Letters* 19 (10) (2013) 3047–3050.
- [30] M. S. Ismail, M. Moghavvemi, T. M. I. Mahlia, Characterization of pv panel and global optimization of its model parameters using genetic algorithm, *Energy Conversion and Management* 73 (9) (2013) 10–25. doi:10.1016/j.enconman.2013.03.033.
- [31] A. Tofighi, Performance evaluation of pv module by dynamic thermal model, *Journal of Power Technologies* 93 (2) (2013) 111–121.
- [32] J. M. Lopez-Guede, J. A. Ramos-Hernanz, M. Grana, Artificial neural network modeling of a photovoltaic module, in: *International Joint Conference SOCO'13-CISIS'13-ICEUTE'13*, Vol. 239 of *Advances in Intelligent Systems and Computing*, 2014, pp. 389–397.
- [33] Schott ase-300-dgf pv panel data sheet, Affordable Solar website.  
URL [http://www.affordable-solar.com/admin/product\\_doc/Doc\\_pd-00-009-c\\_ase\\_300\\_20080328114646.pdf](http://www.affordable-solar.com/admin/product_doc/Doc_pd-00-009-c_ase_300_20080328114646.pdf)
- [34] A. Keyhani, M. N. Marwali, M. Dai, *Integration of Green and Renewable Energy in Electric Power Systems*, Wiley, 2010.
- [35] G. M. Masters, *Renewable and Efficient Electric Power Systems*, John Wiley & Sons Ltd, 2004.
- [36] A. Keyhani, *Design of Smart Power Grid Renewable Energy Systems*, John Wiley & Son, Inc. and IEEE Publication, 2011.
- [37] R. A. Messenger, J. Ventre, *Photovoltaic Systems Engineering*, 2nd Edition, CRC Press, 2003.
- [38] L. Castaner, S. Silvestre, *Modelling Photovoltaic Systems Using PSpice*, John Wiley & Sons Ltd, 2002.
- [39] M. A. Green, *Solar Cells: Operating Principles, Technology, and System Applications*, Prentice Hall Inc., 1982.
- [40] G. R. Walker, Evaluating mppt converter topologies using a matlab pv model, in: *Australasian Universities Power Engineering Conference, AUPEC'00*, Brisbane, 2000.
- [41] A. El Shahat, H. El Shewy, Pm synchronous motor control strategies with their neural network regression functions, *Journal of Electrical Systems* 5 (4).
- [42] S. A. Kalogirou, Optimization of solar systems using neural-networks and genetic algorithms, *Appl Energy* 77 (4) (2004) 383–405.
- [43] S. A. Kalogirou, M. Bojic, Artificial neural networks for the prediction of the energy consumption of a passive-solar building, *Energy* 25 (2000) 479–91.
- [44] A. El Shahat, H. El Shewy, High speed pm synchronous motor basic sizing neural regression function for renewable energy applications, in: Paper ID: X304, 2nd International Conference on Computer and Electrical Engineering (ICCEE 2009), Dubai, UAE, 2009.
- [45] A. El Shahat, Generating basic sizing design regression neural function for hspmsm in aircraft, in: EP-127, 13th International Conference on Aerospace Science & Aviation Technology (ASAT 2009), Military Technical College, Cairo, Egypt, 2009.
- [46] A. El Shahat, H. El Shewy, Neural unit for pm synchronous machine performance improvement used for renewable energy, in: *The Third Ain Shams University International Conference on Environmental Engineering (ASCEE-3)*, Cairo, Egypt, 2009.
- [47] A. El Shahat, H. El Shewy, Neural unit for pm synchronous machine performance improvement used for renewable energy, in: *Global Conference on Renewable and Energy Efficiency for Desert Regions (GCREEDER2009)*, Amman, Jordan, 2009.
- [48] A. R. Conn, N. I. M. Gould, P. L. Toint, A globally convergent augmented lagrangian algorithm for optimization with general constraints and simple bounds, *SIAM Journal on Numerical Analysis* 28 (2) (1991) 545–572.
- [49] A. R. Conn, N. I. M. Gould, P. L. Toint, A globally convergent augmented lagrangian barrier algorithm for optimization with general inequality constraints and simple bounds, *Mathematics of Computation* 66 (217) (1997) 261–288.
- [50] D. E. Goldberg, *Genetic Algorithms in Search, Optimization, and Machine Learning*, Addison Wesley, 1989.
- [51] G. Rudolph, Convergence analysis of canonical genetic algorithms, *Neural Networks, IEEE Transactions on* 5 (1) (1994) 96–101.
- [52] J. H. Holland, *Adaptation in Natural and Artificial Systems*, Ann Arbor, Univ. of Michigan Press, 1995.
- [53] G. Cvetkovski, L. Petkovska, M. Cundev, S. Gair, Mathematical model of a permanent magnet axial field synchronous motor for ga optimisation, in: *Proc. ICEM'98*, Vol. 2/3, 1998, pp. 1172–1177.
- [54] A. El Shahat, A. Keyhani, H. El Shewy, Spacecraft flywheel high speed pm synchronous motor design (classical & genetic), *Journal of Theoretical and Applied Information Technology* 13 (1) (2010) 83–100.
- [55] A. El Shahat, H. El Shewy, Pm synchronous motor genetic algorithm performance improvement for renewable energy applications, in: MDGEN11, Accepted in the International Conference on Millennium Development Goals (MDG): Role of ICT and other technologies, Chennai, India, 2009.
- [56] A. El Shahat, H. El Shewy, Pm synchronous motor genetic algorithm performance improvement for green energy applications, in: Paper ID: X792, Accepted in 2nd International Conference on Computer and Electrical Engineering (ICCEE 2009), Dubai, UAE, 2009.